Basalt Fiber Reinforced and Elastomer Toughened Polylactide Composites: Mechanical Properties, Rheology, Crystallization, and Morphology

Tao Liu, Fengmei Yu, Xuejiang Yu, Xiuli Zhao, Ai Lu, Jianhua Wang

Institute of Chemical Materials, China Academy of Engineering Physics, Mianyang 621900, People's Republic of China

Received 16 February 2011; accepted 27 May 2011
DOI 10.1002/app.34995
Published online 8 January 2012 in Wiley Online Library (wileyonlinelibrary.com).

ABSTRACT: A series of the reinforced and toughened polylactide (PLA) composites with different content of basalt fibers (BF) were prepared by twin screw extruder. The toughness of BF/PLA composites was improved further by the addition of polyoxyethylene grafted with maleic anhydride (POE-*g*-MAH), ethylene–propylene–diene rubber grafted with maleic anhydride (EPDM-*g*-MAH), and ethylene-acrylate-glycidyl methacrylate copolymer (EAGMA), relatively. The mechanical properties, rheology, crystallization, and morphology of BF/PLA composites were studied. The results showed that basalt fiber had significant reinforcing and toughening effect in comparsion with glass fiber. EAGMA was more effective in toughening BF/PLA composites than POE-*g*-MAH and EPDM-*g*-MAH. When the content of EAGMA achieved to 20 wt %, the impact strength of BF/PLA/EAGMA composite increased to 33.7 KJ/m^2, meanwhile the value was improved by 71.1% compared with pure PLA. According to dynamic rheometer testing, the use of the three kinds of elastomers increased the melt dynamic viscosity. Differential scanning calorimetry analysis showed that POE-*g*-MAH and EPDM-*g*-MAH can decrease the cold crystallization temperature (T_{cc}) to approximately 20°C and dramatically improve crystallinity (χ_c) of BF/PLA composites. © 2012 Wiley Periodicals, Inc. J Appl Polym Sci 125: 1292–1301, 2012

Key words: polylactide; basalt fiber; mechanical properties; crystallization

INTRODUCTION

Recently, demands for biodegradable polymers with excellent material properties have been growing at a rapid rate. In recent years, polylactide (PLA) has been one of the most promising candidates because of the possibility of producing from annually renewable resources and its degradability to natural samples in a short period of time in contrast with conventional plastics.[1–5] However, some problems of PLA exist in applications such as the toughness and thermal stability. For example, PLA can be synthesized from direct condensation of lactic acid and by ring-opening polymerization of the cyclic lactide dimer. Of the two isomers available (D- and L-), the polymer of the L-enantiomorph is a hard, transparent, and highly crystalline polymer. Relatively large spherulites are achievable as a result of slow crystallization and as a consequence, brittleness can occur.

To solve the problem of brittleness of PLA, a variety of fibers have been used with some success, including natural fibers, man-made fibers based on renewable raw materials.[6–15] For example, Ochi[6] investigated kenaf/PLA composites with the content of different fiber, and found that tensile and bending strength as well as Young's modulus increased linearly up to a fiber content of 50%. Hu and Lim[7] investigated the mechanical properties of compression molded composites with different volume fractions and the effects of alkali treatment on the fiber surface morphology of hemp. They found that the best mechanical properties of composites were obtained with 40% volume fraction of alkali-treated fiber bundles. Oksman et al.[8] studied the effect of flax fiber on mechanical properties of flax/PLA composites, and found that the stiffness of PLA increased from 3.4 to 8.4 GPa with an addition of 30 wt % flax fibers. Tokoro et al.[9] examined three kinds of injection molded bamboo fiber (short fiber bundles, alkali-treated fiber bundles, and steam-exploded fiber bundles) reinforced PLA, and found that the highest bending strength was obtained with steam-exploded fibers. Ganster and Fink[10] investigated injection molded Cordenka fiber-reinforced PLA with a fiber mass content of 25%, and found that stiffness and strength of the composites could be approximately doubled compared with the pure

Correspondence to: X. L. Zhao (zhxl75@163.com) or J. H. Wang (Wangjh_caep@163.com).

Contract grant sponsor: Science and Technology Development Foundation of China Academy of Engineering Physics; contract grant number: 2008A0302012.

matrix, and the impact strength could be tripled. Although a lot of literatures reported the mechanical behavior of various fiber/PLA composites in detail, there are less articles systematically on the basalt fiber reinforced PLA composites.

Basalt fiber extruded from melted basalt rock reportedly possesses at least 16% higher modulus, equivalent tensile strength, and higher alkaline resistance compared with glass fiber, enhanced interfacial adhesion and are available commercially.[16–18] Moreover, high heat resistance, high stability in aggressive media, substantial sound absorption, and enormous physical durability of basalt fiber results in glass fiber replacement in fields of modified polymers. For example, Milan et al.[18] found that the properties of recycled PET were significantly enhanced by the 20 and 30% filling with basalt fibers. Botev et al.[19] investigated the basalt fiber reinforced the PP composites, and found that the impact strength of the composites with different basalt content had the same value (25–26 J/m), which was about four times higher than that of unfilled PP (6 J/m). Pierre et al.[20] prepared the pressure piping by basalt fiber reinforced polymer composite, and found that basalt fiber reinforcement had improved strength properties over contemporary E-glasses fiber for a range of loading scenarios. From the examples, one can see that the properties of polymer were dramatically improved with basalt fiber. So it is necessary to systematically study the properties of basalt fiber reinforced PLA composites.

In this article, a series of the reinforced and toughened BF/PLA composites were prepared by twin screw extruder. We can systematically investigate the effect of content of basalt fiber on the mechanical properties, rheology, crystallization, and morphology of BF/PLA composites. Meanwhile, three kinds of elastomers such as ethylene–propylene–diene rubber grafted with maleic anhydride (EPDM-*g*-MAH), polyoxyethylene grafted with maleic anhydride (POE-*g*-MAH), and ethylene-acrylate-glycidyl methacrylate copolymer (EAGMA), were selected as the flexibilizer to further toughen BF/PLA composites.

EXPERIMENTAL

Materials and preparation

PLA resin (AL-1001, L/D was about 96.1/3.9) was supplied by Shenzhen BrightChina Industrial Co. Ltd., China. The weight-average (M_w) molecular weight of PLA was 122,398 g/mol, and M_w/M_n was equal to 1.4 by the measurement of waters 2414/1515 gel permeation chromatography (USA). Basalt fiber (GBF9-800) was supplied by Dongguan Russia and Gold Basalt Fiber Co. Ltd., China. Glass fiber (ECT5301HP-2200) was supplied by Chongqing Polymer Composite International, China. Silane resin acceptor (KH550) was a commercial product of Nanjing Yudeheng Fine Chemical Co. Ltd., China. Ethylene–propylene–diene rubber grafted with maleic anhydride (9802) and polyoxyethylene grafted with maleic anhydride (9805) were supplied by Shanghai Sunny New Technology Development Co. Ltd., China. Ethylene-acrylate-glycidyl methacrylate copolymer (AX 8900) was supplied by Arkema Inc, France. Antioxygen (Irganox 168 and 1098) was supplied by BASF chemical company, Germany.

The PLA resin was dried at 80°C for 6 h to remove residual moisture. The PLA resin, silane resin acceptor, elastomer, and antioxygen were mixed in a high-speed blender for 1 min, and then were processed in a PTW252 twin-screw extruder (HAAKE, Germany) to give samples. The rotational speed of the extruder was 90 rpm, and the temperatures of its eight sections, from the charging hole to the ram head, were150, 150, 155, 160, 165, 160, 155, and 150°C. The samples were dried at 80°C for 8 h to remove moisture, and then were injected to standard testing samples (the length of the basalt fiber in the samples was less than 1 mm by the blending and injection-molding processes). The injection barrel temperature profile was set to 165, 170, 170, and 175°C. The mold temperature was kept at 30°C.

Mechanical testing

The tensile and flexural properties of the samples were carried out with a 5582-SP1376 Instron instrument (USA) according to ISO 527 and ISO 178, relatively. The crosshead speed was for tensile measurements 5 mm/min, and the strain rate for tensile was 3.33×10^{-3} s^{-1}. The crosshead speed for flexural measurements 2 mm/min, and the strain rate for flexural was 1.37×10^{-4} s^{-1}. The testing of unnotched charpy impact of the samples were carried out with ZBC1400-2 impact testing machine (China) according to ISO 179/1eU. All tests were carried out in an air-conditioned room (25°C).

Dynamic rheology analysis

Viscoelastic characterization of melt of the composites was conducted with RS600 rotational rheometer (HAAKE). The linear viscoelastic range of deformation was obtained by a strain sweep test. The response to applied oscillatory deformation at 170°C was evaluated in the frequency range of 0.01 to 100 Hz.

Differential scanning calorimetry (DSC) analysis

The crystallization behavior of PLA and its composites were performed in a nitrogen atmosphere by

use of a DSC-6 Perkin–Elmer differential scanning calorimeter (DSC). The crystallization exotherm was recorded when the samples (about 9 mg) were heated from 20 to 200°C and were held at that temperature for 5 min to erase the thermal history, and then cooled to 20°C at the different rate of 10, 20, 50, and 100°C/min. The samples were reheated to 200°C at a rate of 10°C/min.

Scanning electron microscope (SEM)

Samples were cryogenically fractured in liquid nitrogen and observed with a scanning KYKY 2800 scanning electron microscope.

RESULTS AND DISCUSSION

Mechanical properties

Figure 1 shows the curves of the mechanical properties versus the content of fiber for the BF/PLA and GF/PLA composites. As shown in Figure 1, the mechanical properties of BF/PLA composites are obviously higher than those of GF/PLA composites at the same content of fiber. This implies that the basalt fiber exhibits better tensile strength and modulus than the glass fiber, so basalt fiber can act as better excellent reinforcing effect. At the same time, the tensile strength and flexural strength of BF/PLA composites increase from 58.3 MPa to 110.2 MPa, and from 90.4 MPa to 147.8 MPa as the content of basalt fiber increased from 0 to 40 wt %, respectively. The impact strength of BF/PLA composites increases to the maximum value 24.6 KJ/m^2 and then decreases to the minimum value 20.2 KJ/m^2, but the minimum value still exhibits higher impact strength than that of pure PLA. So this proves that the basalt fiber shows reinforcing and toughening effects in the BF/PLA composites.

Three kinds of elastomers were selected as the flexibilizer so that the toughness of BF/PLA composites were improved further. Figure 2 shows the curves of the mechanical properties versus the content of elastomer for the BF/PLA/elastomer composites. We knew that the impact strength of BF/PLA composites achieved the maximum value when the content of basalt fiber got to 20 wt % from Figure 1. Therefore, the content of basalt fiber was fixed at 20 wt % in this study. It is well known that with increasing the content of elastomer, the brittle-ductile transition temperature shifted to lower temperatures promoting the toughness.[21] As expected there is an increase in the toughening of BF/PLA composites after the addition of EAGMA, which is proportional to the content of EAGMA as seen in Figure 2. Impact strength of BF/PLA/EAGMA composites achieve to the maximum value 33.7 KJ/m^{2}with 20 wt % EAGMA content, and the value is improved by 37.0% compared with BF/PLA composites. This is probably that EAGMA is a copolymer of core-shell structure.[22–24] An elastomeric arcylate acts as core, and glycidyl methacrylate acts as shell. The carboxyl and hydroxyl groups in PLA react with the epoxy group from glycidyle methacrylate in the melt state,[25] so the shell has a good reactive compatibility

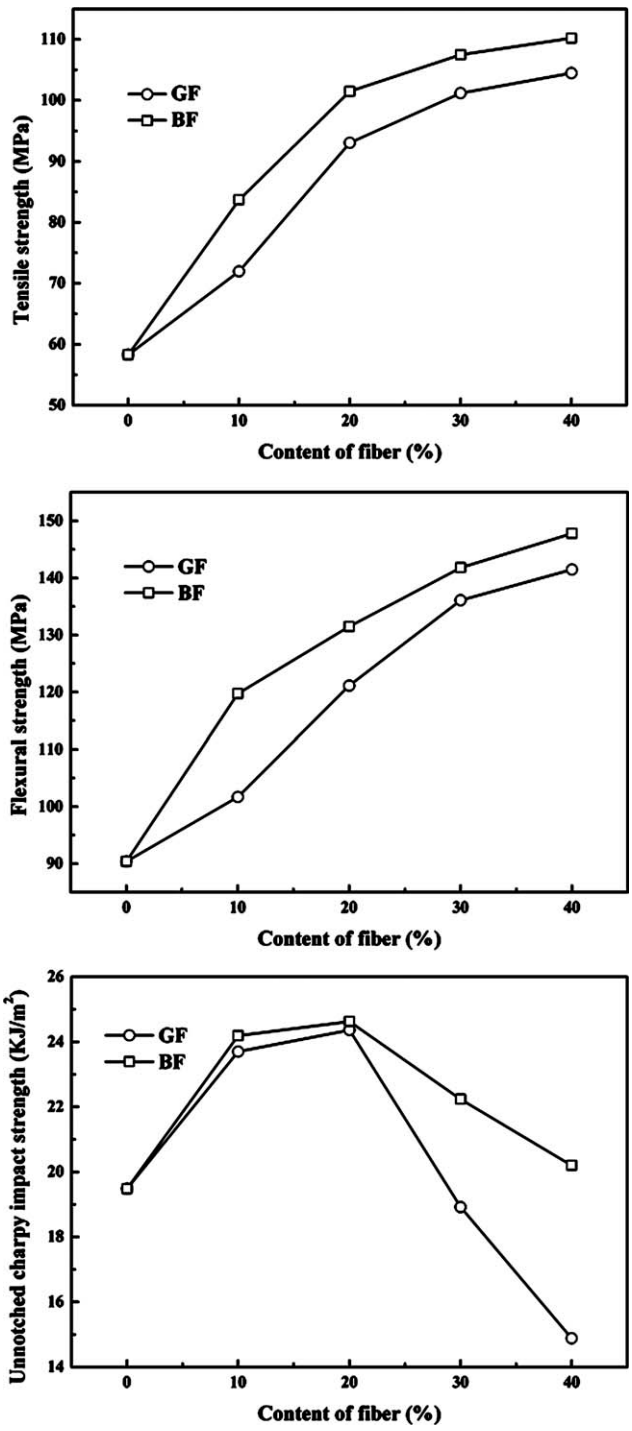

Figure 1 Curves of the mechanical properties versus the content of fiber for BF/PLA and GF/PLA composites.

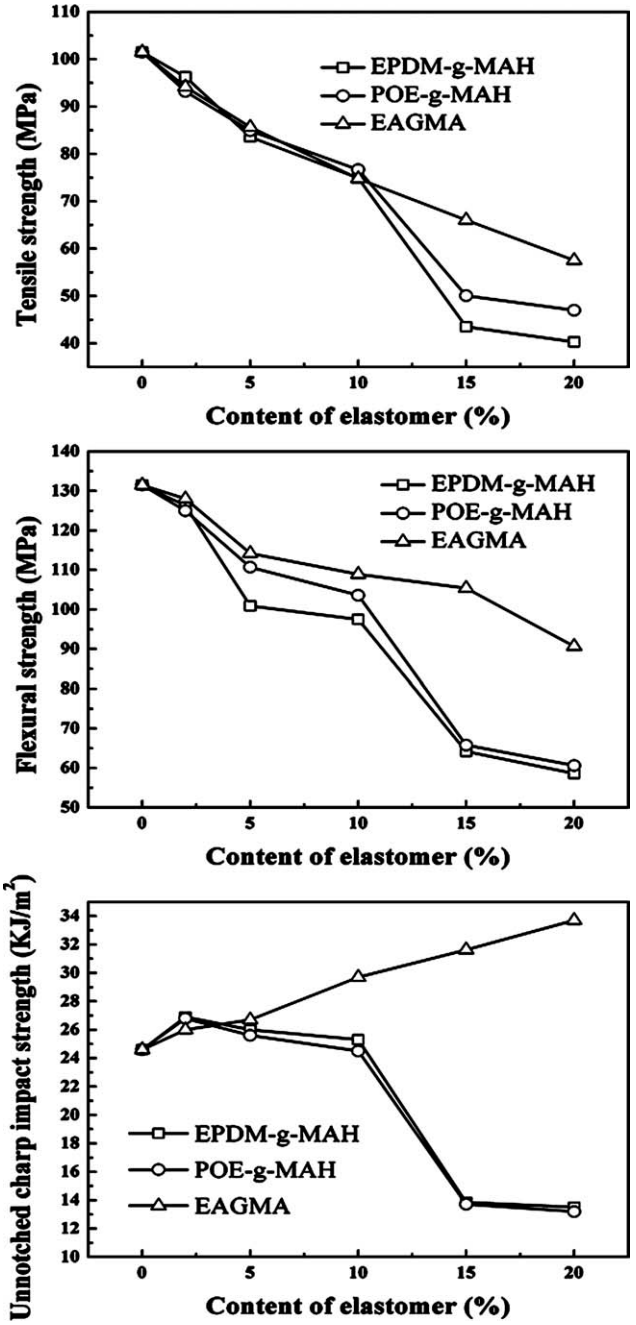

Figure 2 Curves of the mechanical properties versus the content of elastomer for BF/PLA/elastomer composites.

with PLA, and the core toughens the PLA. However, we expected that the situation that the toughness of the BF/PLA/elastomer composites increased with the growth of the content of EPDM-*g*-MAH and POE-*g*-MAH did not occur. Actually, BF/PLA/EPDM-*g*-MAH and BF/PLA/POE-*g*-MAH composites with 2 wt % elastomer content exhibit the maximum impact strength. Especially, when the content of EPDM-*g*-MAH and POE-*g*-MAH are more than 10 wt %, impact strength dramatically decline. This is probably that the influence of the particle size of elastomers on the impact strength of BF/PLA/elastomer composites. Wu[26] and Cho et al.[27] concluded that the optimum dimension range of the particle size, to achieve maximum resistance to crack propagation, must be some critical size. Larger rubber particles have a negative influence on the toughening. With the growth of the content of EPDM-*g*-MAH and POE-*g*-MAH, the particle size of BF/PLA/elastomer composites maybe increase, which leads to a decrease of impact strength beyond elastomer content 2 wt %.

The tensile strength and flexural strength of BF/PLA/elastomer composites decline with the content of elastomer, but the tensile strength and flexural strength of BF/PLA/EAGMA composites with 20 wt % EAGMA content still achieve 57.5 MPa and 90.7 MPa, respectively. These values are very approximate to the tensile strength and flexural strength of pure PLA. So we conclude that EAGMA shows much better toughening effects for the BF/PLA composites than did POE-*g*-MAH and EPDM-*g*-MAH, relatively.

Rheologic behavior

Figure 3 shows the relationship of the dynamic viscosity and frequency for BF/PLA and BF/PLA/elastomer composites. As shown in Figure 3, the dynamic viscosity of the BF/PLA and BF/PLA/elastomer composites decrease with increasing frequency. However, the addition of POE-*g*-MAH, EPDM-*g*-MAH, and EAGAM increases the dynamic viscosity of BF/PLA composite. POE-*g*-MAH, EPDM-*g*-MAH, and EAGAM are elastic with high viscosity and good elasticity values, so the introduction of elastomers improves the melt strength and dynamic viscosity of the BF/PLA composite. As reported by Busse,[28] the better the melt elasticity of polymer is, the higher the melt strength is. Meanwhile, Figure 4 shows the curves of dynamic

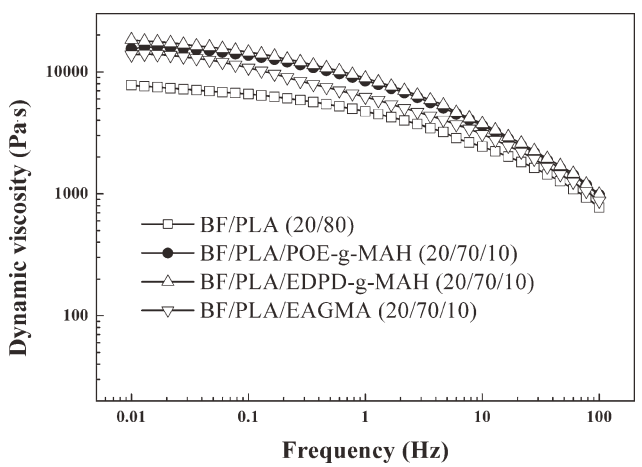

Figure 3 Curves of dynamic viscosity versus frequency for BF/PLA and BF/PLA/elastomer composites.

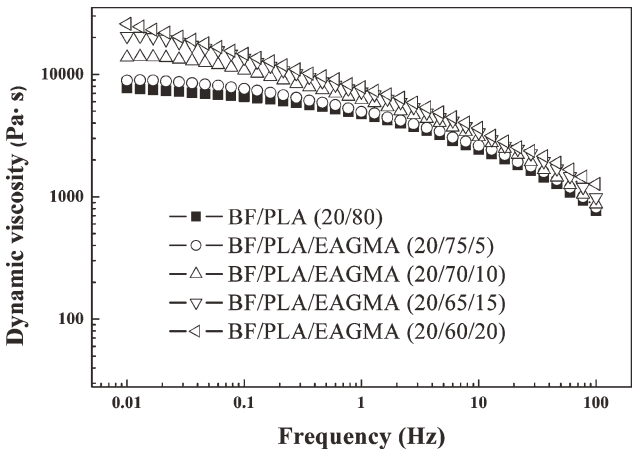

Figure 4 Curves of dynamic viscosity versus frequency for the different content of EAGMA in BF/PLA/EAGMA composites.

viscosity versus frequency for the different content of EAGMA in BF/PLA/EAGMA composites. From the Figure 4 one can see that the dynamic viscosity of the BF/PLA/EAGMA composites increase with the growth of the content of EAGMA.

Figure 5 shows the storage modulus and loss modulus with frequency for BF/PLA and BF/PLA/

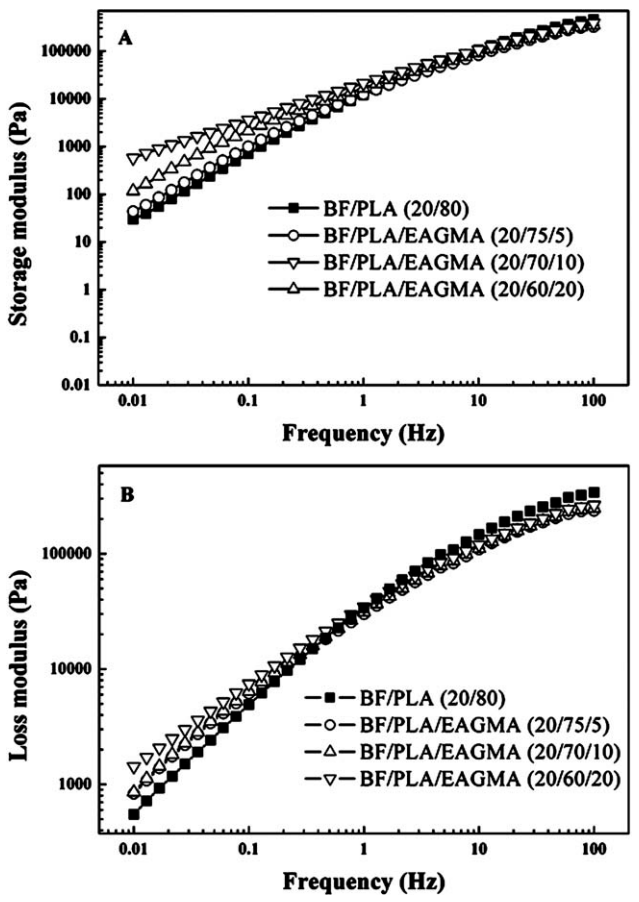

Figure 5 Curves of dynamic modulus versus frequency for BF/PLA and BF/PLA/AEGMA composites.

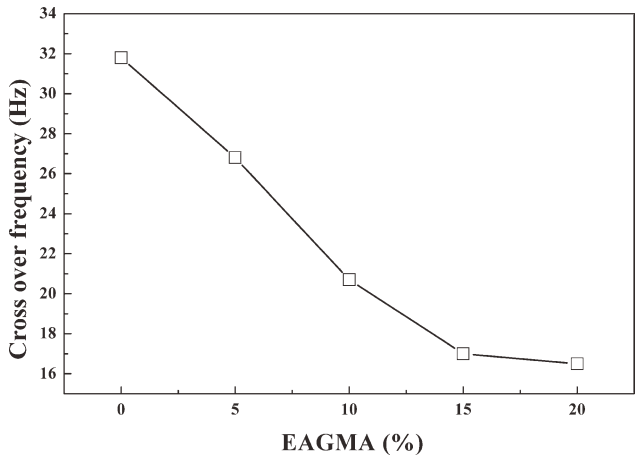

Figure 6 Curves of crossover frequency versus content of EAGMA for BF/PLA and BF/PLA/EAGMA composites.

EAGMA composites. The storage modulus G' and loss modulus G'' [Fig. 5(A,B)] exhibits similar trend. At low frequencies, the qualitative behavior of storage modulus of BF/PLA/EAGMA composites increases for presence of EAGMA which is related to the melt elasticity enhancement. The stronger the hydrodynamic effect in the melt, the more is the upturn of modulus as evidenced by relevant graphs in Figure 5(A),[29] whereas at high frequencies, the qualitative behavior of storage modulus of BF/PLA/EAGMA composites decreases when compared with BF/PLA composite.

The restricted molecular mobility can also be traced by crossover point characteristic at which the values of G' and G'' are equal. By increasing the angular frequencies, the crossover point indicates a transition from a more viscous deformation to a more elastic behavior. The shift in crossover frequency represents the changes in molecular mobility and relaxation time behavior. As seen in Figure 6, the crossover frequency of composites decreases

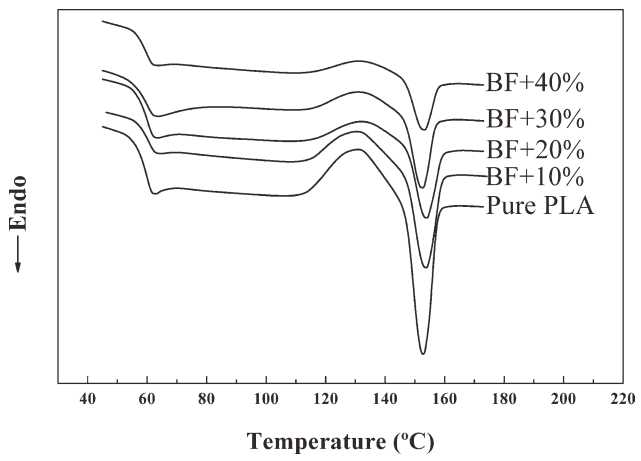

Figure 7 DSC curves of PLA and BF/PLA composites in heating process.

TABLE I
DSC Characterization of PLA and BF/PLA Composites

Sample	T_{cc} (°C)	ΔH_{cc} (J/g)	T_m (°C)	ΔH_m (J/g)	χ_c (%)
Pure PLA	131.44	10.92	152.80	10.26	10.95
10 wt % BF	131.84	6.88	153.38	7.17	8.50
20 wt % BF	132.87	4.54	153.83	4.83	6.44
30 wt % BF	133.85	3.61	152.82	4.02	6.13
40 wt % BF	133.36	3.21	152.79	3.35	5.96

with the growth of content of EAGMA. This is because the EAGMA affects the molecular mobility of the PLA matrix. The molecular chain of PLA grafted the EAGMA by reactivity of the carboxyl and hydroxyl with the epoxy group.[25] However, EAGAM are elastic with high viscosity, which causes the molecular chain of EAGMA to move relatively slower than the molecular chain of PLA. Therefore, addition of EAGMA restricts the mobility of molecular chain of PLA. Meanwhile the restriction in molecular mobility is more significant with the increasing of content of EAGMA.[29,30]

DSC analysis

Figure 7 shows the DSC curves of PLA and BF/PLA composites in heating process, and the resulting parameters are shown in Table I. By considering the melting enthalpy of 100% crystalline polylactide as 93.7 J/g,[31] the crystallinity (χ_c) is calculated according to the following formula:

$$\chi_c = \frac{\Delta H_m}{(1-\Phi)\times 93.7}\times 100\% \quad (1)$$

where ΔH_m is the melting enthalpy of sample and Φ is the content of filler in PLA composites.

From Table I, a slightly increase of the cold crystallization temperature (T_{cc}) of BF/PLA composites can be observed with the increasing of content of basalt fiber, whereas the melting enthalpy (ΔH_m), crystallization enthalpy (ΔH_{cc}) and χ_c decreases. These results indicate that basalt fiber affects the molecular mobility of the PLA matrix. Furthermore, it is obvious that the decrease of crystallinity contributes to increasing the impact strength of the hybrid composite, since the flexibility of molecular chains declines for increasing the crystallinity.[32]

Figure 8 DSC curves of BF/PLA and BF/PLA/elastomer composites in heating process, and the resulting parameters are shown in Table II. As shown in Table II, the addition of EAGMA, POE-*g*-MAH, and EPDM-*g*-MAH shows the effects on the crystallization behavior of BF/PLA composite. Compared with the BF/PLA composite, the presence of POE-*g*-MAH and EPDM-*g*-MAH results in the value of T_{cc} decreasing to an approximately 20°C, but the values of χ_c is about more four times than its of BF/PLA composite. These results indicate that the introduction of POE-*g*-MAH and EPDM-*g*-MAH promote the crystallization of BF/PLA composite. This is because the elastic particles of POE-*g*-MAH and EPDM-*g*-MAH act as nucleating agents for PLA in its BF composites since there are obvious cold crystallization exotherm peak, which results in brittleness of the composites, so these two elastomers can not improve the toughness of BF/PLA composites. In contrast, EAGMA restricts the molecular mobility of PLA and causes larger percentage of amorphous phase to form, and the toughness of BF/PLA composites is further improved. A similar result is found in PBT/PC/EBAGMA and PBT/PC/POE blends by Bai et al.[33] It is reported that EBAGMA could interfere with PBT crystallization and causes a greater fraction of amorphous PBT in PBT/PC/EBAGMA blends, whereas POE could promote the crystallization of PBT in PBT/PC/POE blends. Meanwhile, the melting curves of BF/PLA/POE-*g*-MAH and BF/PLA/EPDM-*g*-MAH composites change to the bimodal. The different of cooling rate of BF/PLA/EPDM-*g*-MAH composites in DSC measurements were done to research on the effect of the cooling cycle of the thermal analysis on the melting curves. As shown in Figure 9 and Table III, the peak shape of the melting curves, T_{cc} and χ_c of BF/PLA/EPDM-

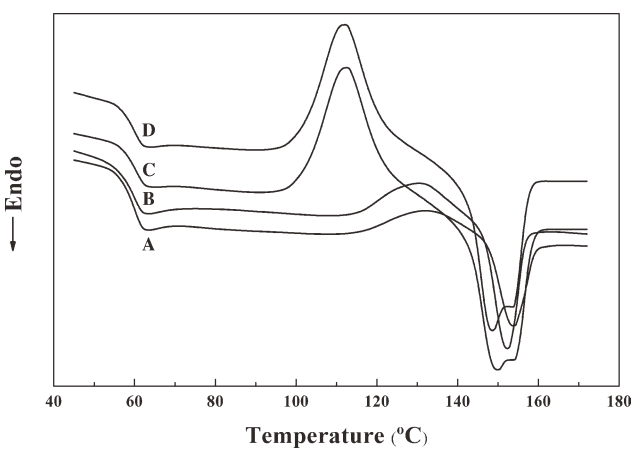

Figure 8 DSC curves of BF/PLA and BF/PLA/elastomer composites in heating process. (A) BF/PLA (20/80), (B) BF/PLA/EAGMA (20/70/10), (C) BF/PLA/POE-*g*-MAH (20/70/10), and (D) BF/PLA/EPDM-*g*-MAH (20/70/10).

TABLE II
DSC Characterization of BF/PLA and BF/PLA/Elastomer Composites

Sample	T_{cc} (°C)	ΔH_{cc} (J/g)	T_m (°C)	ΔH_m (J/g)	χ_c (%)	BF (%)
None	132.87	4.54	153.83	4.83	6.44	20
10 wt % EAGMA	131.62	5.78	152.26	6.21	9.47	20
10 wt % POE-*g*-MAH	112.97	16.84	149.83	17.86	27.23	20
10 wt % EPDM-*g*-MAH	112.37	17.77	148.55	17.04	25.98	20

g-MAH composites at the different of cooling rate are nearly unchanged, which proves that the cooling cycle of the thermal analysis is not direct reason that the melting curves of BF/PLA/EPDM-*g*-MAH composites change to the bimodal. This is probably that the secondary crystallization occurs during the crystallization of BF/PLA/EPDM-*g*-MAH composites.

Morphology

The mechanical properties of reinforced materials are closely related to the intrinsic characteristics of both the matrix and fiber and to the nature of the fiber/matrix interface.[34–36] Figure 10 displays the overall SEM micrographs of the cryofracture surface morphology of the BF/PLA and BF/PLA/elastomer composites. As shown in Figure 10(A), the fractured surface is flat, which is the evidence of brittle break. On the other hand, the fiber surface is relatively smooth, and no gap around the fibers was observed. This indicates that the basalt fiber is strongly bonded to the PLA matrix, which results from the reactivity of the carboxyl group of PLA and the amine group of the silane coupling agent coated on the basalt fibers.[37] Even though the interface of fibers and PLA matrix is good, the BF/PLA composite appears to be brittle due to the very poor toughness of the PLA matrix. Figure 10(B–D) shows the SEM micrographs of the BF/PLA/POE-*g*-MAH, BF/PLA/EPDM-*g*-MAH, and BF/PLA/EAGMA composites, respectively. As shown, not only do the BF/PLA/elastomers composites fracture in tough manner but also some similar spherical traces are also observed in Figure 10(B,C). Ductile fracture indicates that the incorporation of 10 wt % POE-*g*-MAH, EPDM-*g*-MAH, and EAGMA can improve the toughness of the BF/PLA composites. But in actual mechanical properties process, impact strength of BF/PLA/POE-*g*-MAH and BF/PLA/EPDM-*g*-MAH composites have no obvious improvement in comparison with BF/PLA composite. For this reason we examined the situation of the dispersed elastomer phase.[26,27] As shown in Figures 11 and 12, with the growth of POE-*g*-MAH and EPDM-*g*-MAH content, the particle size obviously increased, which results in the toughness of BF/PLA/POE-*g*-MAH and BF/PLA/EPDM-*g*-MAH composites decrease.

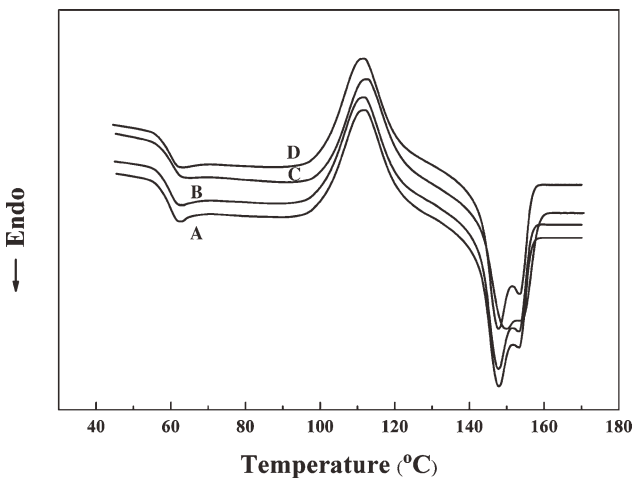

Figure 9 DSC curves of BF/PLA/EPDM-*g*-MAH for the different cooling rate. (A) Cooling rate of 10°C/min, (B) cooling rate of 20°C/min, (C) cooling rate of 50°C/min, and (D) cooling rate of 100°C/min.

Figure 13 SEM micrographs of the cryofracture surface morphology of the BF/PLA/EAGMA composites. As shown in Figure 13, the more the content of EAGMA is, the better the adhesion with basalt fiber and PLA matrix is. A very thin polymer film remains in fiber surface and no debonding is found. On the contrary, with the increasing of content of EAGMA, the fracture surfaces change markedly and exhibited ductile fracture surface morphology, which indicates that the EAGMA can act as the interlayer between the PLA matrix and basalt fiber. This layer relieves the triaxial stress imposed by the plane strain constraint during the impact test. Furthermore, the elastic EAGMA interlayer could deflect the propagation of cracks during impact loading. Such deflections not only dissipate a large amount of the fracture energy but also prevent brittle failure

TABLE III
DSC Characterization of BF/PLA/EPDM-*g*-MAH Composites

Cooling rate	T_{cc} (°C)	ΔH_{cc} (J/g)	T_m (°C)	ΔH_m (J/g)	X_c (%)	BF (%)
10°C/min	111.77	17.48	147.85	16.91	25.78	20
20°C/min	111.75	17.83	147.74	17.08	26.04	20
50°C/min	112.37	17.77	148.55	17.04	25.98	20
100°C/min	111.49	17.35	147.67	16.86	25.71	20

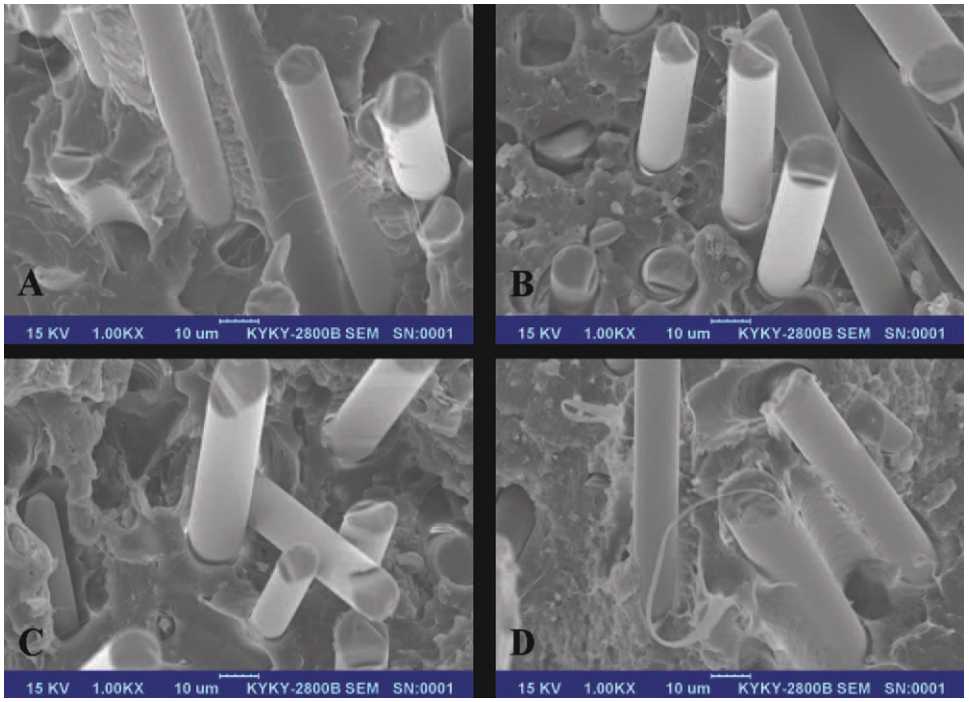

Figure 10 SEM micrographs of the cryofracture surface morphology of the BF/PLA and BF/PLA/elastomer composites. (A) BF/PLA(20/80), (B) BF/PLA/POE-*g*-MAH (20/70/10), (C) BF/PLA/EPDM-*g*-MAH(20/70/10), and (D) BF/PLA/EAGMA (20/70/10). [Color figure can be viewed in the online issue, which is available at wileyonlinelibrary.com.]

for the basalt fiber and basalt fiber/PLA interface.[38,39] The finding was in accordance with the result of impact strength of BF/PLA/EAGMA composites.

CONCLUSIONS

A series of the reinforced and toughened polylactide (PLA) composites with different content of basalt fibers (BF) are prepared by twin screw extruder.

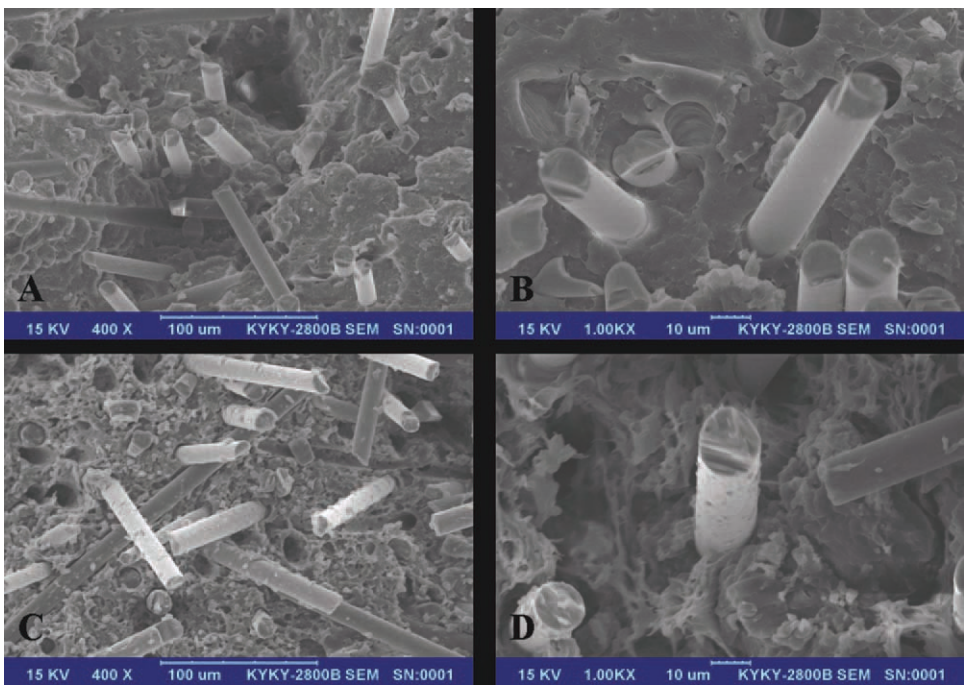

Figure 11 SEM micrographs of the cryofracture surface morphology of the BF/PLA/EPDM-*g*-MAH composites. (A and B) BF/PLA/EPDM-*g*-MAH (20/78/2) and (C and D) BF/PLA/EPDM-*g*-MAH (20/60/20). [Color figure can be viewed in the online issue, which is available at wileyonlinelibrary.com.]

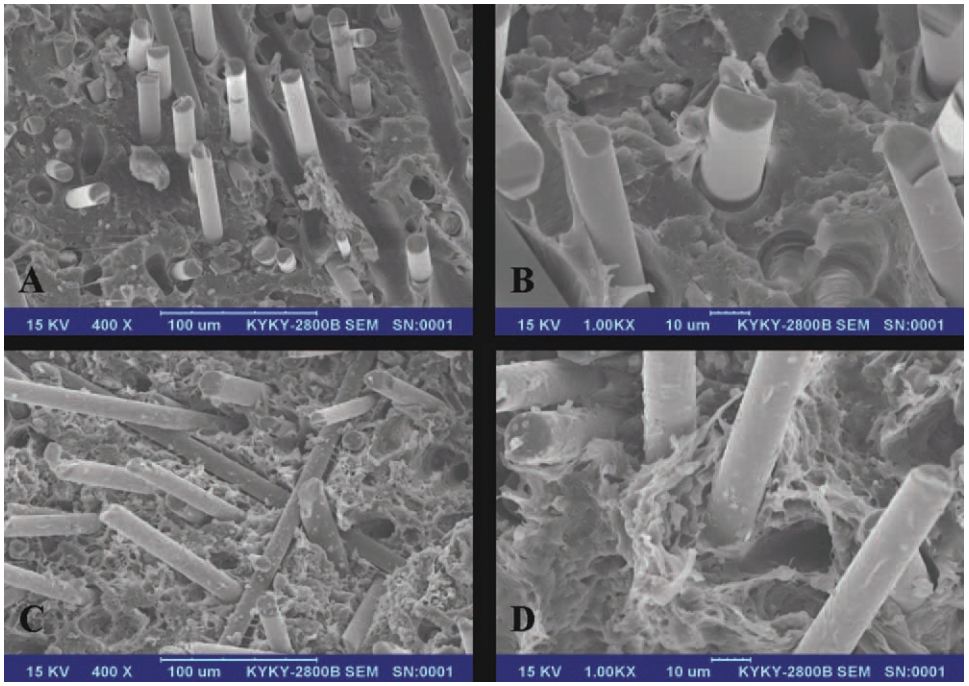

Figure 12 SEM micrographs of the cryofracture surface morphology of the BF/PLA/POE-*g*-MAH composites. (A and B) BF/PLA/POE-*g*-MAH (20/78/2) and (C and D) BF/PLA/POE-*g*-MAH (20/60/20). [Color figure can be viewed in the online issue, which is available at wileyonlinelibrary.com.]

POE-*g*-MAH, EPDM-*g*-MAH, and EAGMA are evaluated for toughening BF/PLA composites. The basalt fiber shows reinforcing and toughening effects in the BF/PLA composites. EAGMA is more effective in toughening BF/PLA composites than POE-*g*-MAH and EPDM-*g*-MAH, which results from its better compatibility with PLA and the stronger adhesion with basalt fiber and PLA. According to

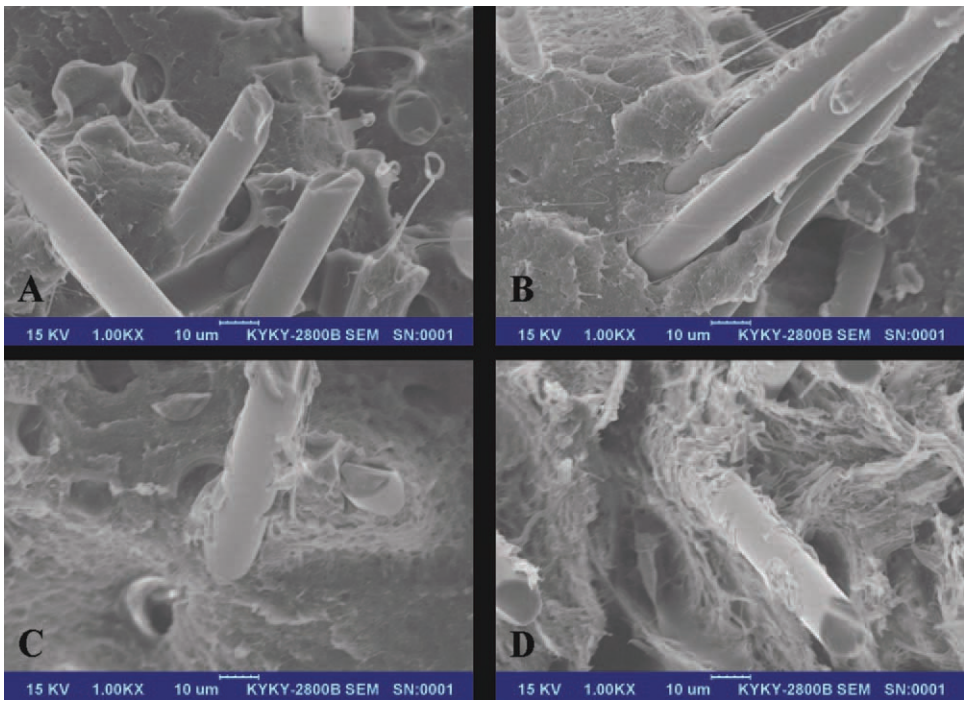

Figure 13 SEM micrographs of the cryofracture surface morphology of the BF/PLA/EAGMA composites. (A) BF/PLA/EAGMA (20/75/5), (B) BF/PLA/EAGMA (20/70/10), (C) BF/PLA/EAGMA(20/65/15), and (D) BF/PLA/EAGMA(20/60/20). [Color figure can be viewed in the online issue, which is available at wileyonlinelibrary.com.]

dynamic rheometer testing, the use of the three kinds of elastomer increases the melt dynamic viscosity. The shift in crossover frequency represents the changes in molecular mobility and relaxation time behavior. The crossover frequency of composites decreased with the growth of content of EAGMA because of the restriction in molecular mobility. Differential scanning calorimetry analysis shows that POE-*g*-MAH and EPDM-*g*-MAH dramatically promote the crystallization of BF/PLA composite and lead to an increase in the crystallization degree and a decrease in T_{cc}. SEM photographs show EAGMA can enhance the adhesion basalt fiber and PLA matrix, and the fracture surfaces change markedly and exhibit ductile fracture surface morphology with the increasing of content of EAGMA.

References

1. Reed, A. M.; Gilding, D. K. Polymer 1981, 22, 494.
2. Kalb, B.; Pennings, A. J. Polymer 1980, 21, 607.
3. Carla, M.; Antonio, M.; Vito, D. N. Macromol Chem 1992, 193, 1599.
4. Tsuji, H.; Ikada, Y. J Appl Polym Sci 1998, 67, 405.
5. Martin, O.; Averous, L. Polymer 2001, 42, 6209.
6. Ochi, S. Mech Mater 2008, 40, 446.
7. Hu, R. H.; Lim, J. K. J Compos Mater 2007, 41, 1655.
8. Oksman, K.; Skrifvars, M.; Selin, J. F. Compos Sci Technol 2003, 63, 1317.
9. Tokoro, R.; Vu, D. M.; Okubo, K.; Tanaka, T.; Fujii, T.; Fujiura, T. J Mater Sci 2008, 43, 775.
10. Ganster, J.; Fink, H. P. Cellulose 2006, 13, 271.
11. Huda, M. S.; Drzal, L. T.; Misra, M.; Mohanty, A. K. J Appl Polym Sci 2006, 102, 4856.
12. Cho, D.; Seo, J. M.; Lee, H. S.; Cho, C. W.; Han, S. O.; Park, W. H. Adv Compos Mater 2007, 16, 299.
13. Lee, S. H.; Wong, S. Compos A 2006, 37, 80.
14. Finkenstadt, V. L.; Liu, L. S.; Willett, J. L. J Polym Environ 2007, 15, 1.
15. Nina, G.; Axel, S.; Herrmann, J. M. Compos A 2009, 40, 810.
16. Lisakovski, A. N.; Tsybulya, Y. L.; Medvedyev, A. A. In The Proceedings of the Fiber Society, Raleigh, NC, May 23–25, 2001.
17. Liu, Q.; Montgomery, T. S.; Richard, S. P. Polym Compos 2006, 27, 475.
18. Milan, K.; Ladislav, P.; Miroslav, S.; Jana, M.; Antonin, S.; Josef, S.; Ivan, F. Polym Compos 2008, 29, 437.
19. Botev, M.; Betchev, H.; Bikiaris, D.; Panayiotou J. J Appl Polym Sci 1999, 74, 523.
20. Pierre, M.; Kulvinder, J.; Mohab, E. J Pressure Vessel Technol 2009, 31, 061407.
21. Van der Wal, A.; Nijhof, R.; Gaymans, R. Polymer 1990, 40, 6031.
22. Lin, K. F.; Shieh, Y. D. J Appl Polym Sci 1998, 2069, 69.
23. Maazouz, A.; Sautereau, H.; Gerard, J. F. Polym Bull 1994, 33, 67.
24. Huang, Y. J.; Wu, J. H.; Liang, J. G.; Hsu, M. W.; Ma, J. K. J Appl Polym Sci 2008, 107, 939.
25. Noriaki, K.; Kazushi, Y.; Yew, W. L.; Supaphorn, T. J Appl Polym Sci 2011, 120, 55.
26. Wu, S. Polymer 1985, 26, 1885.
27. Cho, K.; Yang, J. H.; Yoon, S.; Nair, M. H. S. V. J Appl Polym Sci 2005, 95, 748.
28. Busse, W. F. J Polym Sci Part A-2: Polym Phys 1967, 5, 249.
29. Yousef, J. J Vinyl Additive Technol 2010, 16, 70.
30. Gahleitner, M. Prog Polym Sci 2001, 26, 895.
31. Raya, S. S.; Yamadab, K.; Okamotoa, M.; Ueda, K. Polymer 2003, 44, 857.
32. Huda, M. S.; Drzal, L. T.; Mohanty, A. K.; Misra, M. Compos B 2007, 38, 367.
33. Bai, H. Y.; Zhang, Y.; Zhang, Y. X.; Zhang, X. F.; Zhou, W. J Appl Polym Sci 2006, 101, 54.
34. Ronkay, F.; Czigany, T. Polym Adv Technol 2006, 17, 830.
35. Bergeret, A.; Bozec, M. P.; Quantin, J. C.; Crespy, A. Polym Compos 2004, 25, 12.
36. Frenzel, H.; Bunzel, U.; Haessler, R.; Rompe, G. J Adhes Sci Technol 2000, 14, 651.
37. Cheng, H. Y.; Tian, M.; Zhang, L. Q. J Appl Polym Sci 2008, 109, 2795.
38. Wu, J.; Yu, D.; Chan, C. M.; Kim, J.; Mai, Y. W. J Appl Polym Sci 2000, 76, 1000.
39. Tjong, S. C.; Xu, S. A.; Mai, Y. W. J Appl Polym Sci 2003, 88, 1384.